Two-heteroclinic orbits emerging in the reversible homoclinic pitchfork bifurcation

T. Wagenknecht

Department of Engineering Mathematics, University of Bristol, Bristol BS8 1TR, UK

E-mail: `t.wagenknecht@bristol.ac.uk`

Abstract. We consider reversible and $\mathbb{Z}_2$-symmetric systems of ordinary differential equations (ODEs) that possess a symmetric homoclinic orbit to a degenerate equilibrium. The equilibrium is supposed to undergo a reversible pitchfork bifurcation, controlled by the system's parameter. It has been shown in Wagenknecht (Nonlinearity 15(6), pp. 2097-2119) that a multitude of homoclinic orbits emerges in this bifurcation. In particular, if a coefficient in the normal form of the local bifurcation has the correct sign such that this bifurcation is of eye-type, then globally a *reversible homoclinic pitchfork bifurcation* can be observed. This means, that similar to the local bifurcation in which two new equilibria emerge, two homoclinic orbits to these equilibria bifurcate from the primary homoclinic orbit. In this paper we investigate the emergence of two-homoclinic and two-heteroclinic orbits, that is, orbits making two windings in a neighbourhood of the primary orbit, in this bifurcation. Using a combination of geometrical and analytical techniques we prove the emergence of a family of two-homoclinic orbits to periodic orbits and of a two-heteroclinic cycle between equilibria. The general analysis is illustrated by numerical results for an example system of two second order ODEs.

AMS classification scheme numbers: 37C29, 37C80, 37C10

1. Introduction

In this paper we continue the study of a homoclinic orbit to a degenerate equilibrium in the class of reversible and $\mathbb{Z}_2$-symmetric systems of ordinary differential equations (ODEs). We assume that the equilibrium undergoes a local reversible pitchfork bifurcation in which two additional equilibria emerge, and we are interested in bifurcations from the homoclinic orbit. Earlier studies in [19] have shown that generically one finds a remarkable similarity of the local and global bifurcation, in that at the critical parameter value two homoclinic orbits to the additional equilibria emerge. Consequently, the global scenario has been termed a *reversible homoclinic pitchfork bifurcation* in [19].

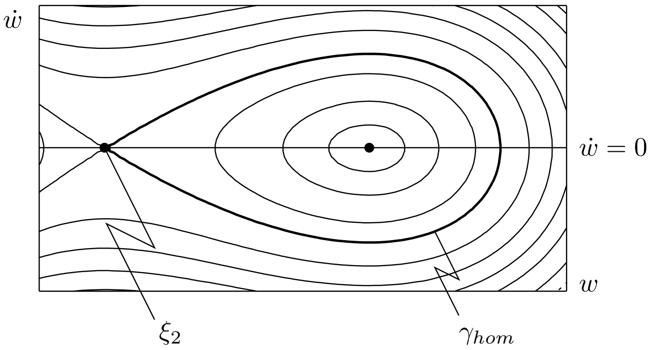

Figure 1. Dynamics of (1) with $\mu = 1$ and $\kappa < 1$ in the space Fix$\,(S)$. A homoclinic orbits γ_{hom} to the equilibrium ξ_2 exists.

Let us introduce this bifurcation using the same numerical example as in [19]. We consider the following system of second order ODEs

$$\begin{array}{rcl} \ddot{v} & = & 2vw + 2\mu v \\ \ddot{w} & = & -v^2 - w^2 + 2\mu w - \kappa \end{array} \tag{1}$$

for $v, w : \mathbb{R} \to \mathbb{R}$, depending on the real parameters μ, κ. This system has been derived in [18] as an unfolding of a degenerate equilibrium with fourfold eigenvalue zero. Note that (1) is reversible with respect to two different linear involutions, which in $(v, \dot{v}, w, \dot{w})$-phase space read

$$R_1 : (v, \dot{v}, w, \dot{w}) \to (v, -\dot{v}, w, -\dot{w})$$

and

$$R_2 : (v, \dot{v}, w, \dot{w}) \to (-v, \dot{v}, w, -\dot{w}).$$

Since R_1 and R_2 commute, the map $S := R_1 \circ R_2$ forms a $\mathbb{Z}_2$-symmetry for (1).

We consider system (1) with $\mu = 1$ under variation of κ only. For $\kappa < 1$ there exists a homoclinic orbit γ_{hom}, which is symmetric with respect to R_1 and R_2 and which is contained in the invariant subspace Fix$\,(S) := \{(0, 0, w, \dot{w})\}$. (As customary we call an orbit of a reversible system symmetric if it is mapped onto itself by the reversing symmetry.) Note that the system within Fix$\,(S)$ is reversible with respect to $R_S : (w, \dot{w}) \to (w, -\dot{w})$. An impression of the phase portrait in the invariant subspace is given in figure 1.

The orbit γ_{hom} undergoes a reversible homoclinic pitchfork bifurcation at $\kappa = -3$. To see this consider the associated equilibrium, which we denote by ξ_2, following the notation in [18, 19]. At $\kappa = -3$ this equilibrium bifurcates in a reversible pitchfork bifurcation in which two additional equilibria ξ_3 and $\xi_4 = R_2\xi_3$ emerge. These equilibria are R_1-symmetric, and they are connected by a heteroclinic cycle. As in [19] we refer to this case as the *eye case* of the pitchfork bifurcation. The global bifurcation of γ_{hom} can be studied numerically using the AUTO/HomCont continuation software, [5]. In figure 2 we present a plot taken from [19]. This figure illustrates the scenario described

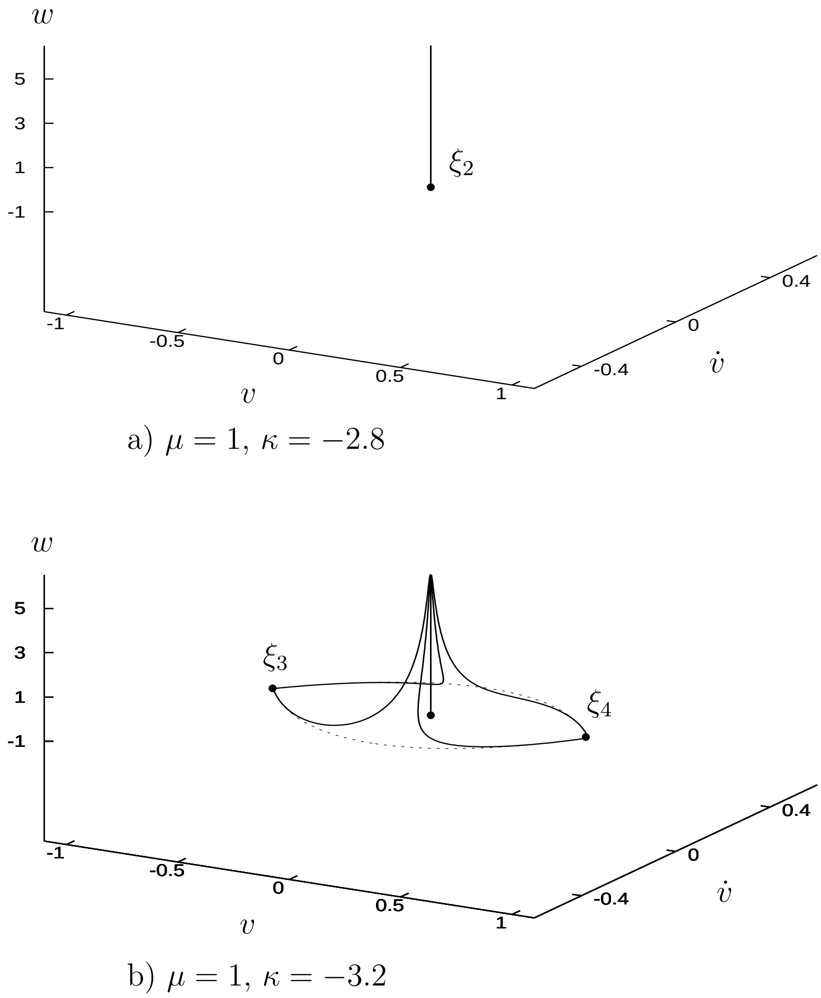

Figure 2. Reversible homoclinic pitchfork bifurcation of γ_{hom}. The figure shows how homoclinic solutions to $\xi_{3,4}$ bifurcate from the primary orbit at $\mu = 1$, $\kappa = -3$. The orbit γ_{hom} is contained in the w-axis because of the chosen projection. Also incorporated is the heteroclinic cycle which is created in the reversible pitchfork bifurcation of ξ_2. Notice the different scales for the $v, \dot{v}$-axes and the w-axis. (Figure taken from [19])

above. At the critical parameter value $\kappa = -3$ not only the equilibrium ξ_2 bifurcates, but so does the orbit γ_{hom} and two additional homoclinic orbits to the outer equilibria ξ_3 and ξ_4 emerge. Note that figure 2 also contains a plot of the (small) heteroclinic cycle that is created in the local bifurcation. All orbits are shown as projections in $(v, \dot{v}, w)$-space.

In [19] we have developed an approach for the analysis of this homoclinic bifurcation. Its main idea is that we do not compute homoclinic orbits to equilibria directly but rather as homoclinic orbits to centre manifolds. These will be orbits which are asymptotic to the centre manifolds in forward and backward time. The manifolds are derived by the use of centre manifold theory and we can detect symmetric homoclinic orbits by studying the intersection of associated centre unstable manifolds with the fixed spaces $\mathrm{Fix}\,(R_i)$. (Note that R_i-symmetric orbits necessarily intersect the space $\mathrm{Fix}\,(R_i)$, [17].) For four-dimensional systems the centre unstable manifolds are three-dimensional and $\dim \mathrm{Fix}\,(R_2) = 2$. Therefore the intersection is generically one-dimensional and consequently a one-parameter family of R_i-symmetric homoclinic orbits to the centre manifolds should exist for each $i \in \{1, 2\}$. It has been proved in [19] that this is indeed the case. Using the invariant foliation of the centre unstable manifolds the asymptotic behaviour of the homoclinic orbits to the centre manifolds could be studied in detail and the generic occurrence of the homoclinic pitchfork bifurcation could be proved.

This follow-up paper to [19] is concerned with the emergence of N-homoclinic orbits in the homoclinic pitchfork bifurcation, that is, homoclinic orbits to the centre manifolds that make N windings in a neighbourhood of the primary orbit. In principle we can follow the above approach and investigate intersections of the centre unstable manifolds with $\mathrm{Fix}\,(R_i)$. Intersections near the equilibrium then yield N-homoclinic orbits with N even, while those 'far away' give rise to N-homoclinic orbits with N odd. Note moreover, that by the same argument as above we can expect the intersection to be one-dimensional such that we can expect one-parameter families of N-homoclinic orbits to the centre manifolds to exist.

For general N it is, however, very difficult to show that the manifolds indeed intersect. We attack this problem for $N = 2$. We introduce a Poincaré map $\mathcal{P}$ from some cross section Σ to the homoclinic orbit to a 'cross section' Σ_0 at the equilibrium. The main difficulty in the analysis of $\mathcal{P}$ lies in describing the behaviour of orbits in a neighbourhood of the centre manifolds where the non-hyperbolicity of the bifurcating equilibrium comes into play. We use generalised Shilnikov variables as introduced by Deng in [3] to overcome this difficulty. This gives us enough information about $\mathcal{P}$ to derive existence results for two-homoclinic orbits to the centre manifold.

We concentrate on parameter values 'after the pitchfork bifurcation' where three equilibria exist. The analysis depends on the behaviour of the strong unstable manifolds of the outer equilibria. Given these manifolds satisfy a certain condition (assumption 4.1) we can prove that for each value of the system's parameter a one-parameter family of symmetric two-homoclinic orbits to the centre manifold exists, see theorem 4.4. Similar to the studies in [19] a refined analysis allows us to determine connecting orbits between equilibria. Theorem 4.5 shows that the two outer equilibria are connected by a two-heteroclinic cycle for all parameter values where they exist.

The paper is organised as follows. In the next section we describe in detail the problem we are interested in. Afterwards, in section 3, we recall results about one-homoclinic orbits from [19] and review the analytical techniques that will be of importance for the detection of two-homoclinic orbits. We then go on to analysing the existence of two-homoclinic orbits to the centre manifolds by introducing the Poincaré map $\mathcal{P}$ in section 4. The analysis of $\mathcal{P}$ leads to the main results of the paper. Afterwards, in section 5 we return to the introductory example (1) and illustrate the general bifurcation results with further numerical experiments on this system.

2. The Problem's Setting

Throughout the paper we consider four-dimensional systems of ODEs

$$\dot{x} = f(x, \lambda), \quad (x, \lambda) \in \mathbb{R}^4 \times \mathbb{R}, \tag{2}$$

with a smooth vector field f, depending on a real parameter λ. We assume that equation (2) is reversible and $\mathbb{Z}_2$-symmetric. More precisely we assume

Assumption 2.1. There exist linear involutions $R_1, R_2 : \mathbb{R}^4 \to \mathbb{R}^4$ with $R_1R_2 = R_2R_1$, $R_1 \neq R_2$, such that $f(R_i\cdot, \cdot) + R_i f(\cdot, \cdot) = 0$, $i = 1, 2$. Moreover, for $\mathrm{Fix}\,(R_i) := \{x : R_i x = x\}$ we have $\dim \mathrm{Fix}\,(R_i) = 2$, $i = 1, 2$.

Under this assumption $S := R_1 \circ R_2$ describes a $\mathbb{Z}_2$-symmetry for equation (2), i.e. we find $f(S\cdot, \cdot) - Sf(\cdot, \cdot) = 0$. In particular, this implies that the space $\mathrm{Fix}\,(S)$ is invariant under the flow of (2). We assume this invariant space to be non-trivial.

Assumption 2.2. For $S = R_1 \circ R_2$ we have $\dim \mathrm{Fix}\,(S) = 2$.

For $x \in \mathrm{Fix}\,(S)$ we find that $R_1 x = R_1R_1R_2 x = R_2 x$, that is, the involutions R_i agree in $\mathrm{Fix}\,(S)$. If we assume that $\mathrm{Fix}\,(R_1) \cap \mathrm{Fix}\,(S) = \{0\}$, then $\mathrm{Fix}\,(-R_1) = \mathrm{Fix}\,(-R_2)$, since $x - R_1 x \in \mathrm{Fix}\,(-R_1) \cap \mathrm{Fix}\,(-R_2)$ for $x \in \mathrm{Fix}\,(S)$. But this would also imply $\mathrm{Fix}\,(R_1) = \mathrm{Fix}\,(R_2)$ and thus $R_1 = R_2$, which results in $S = id$ in contradiction to assumption 2.2. Similarly, it follows that $\mathrm{Fix}\,(R_1) \cap \mathrm{Fix}\,(S) \neq \{0\}$, and therefore a consequence of our assumptions is that

$$\mathrm{Fix}\,(S) = (\mathrm{Fix}\,(R_1) \cap \mathrm{Fix}\,(R_2)) \oplus (\mathrm{Fix}\,(-R_1) \cap \mathrm{Fix}\,(-R_2))\,.$$

We are interested in bifurcations from a symmetric homoclinic orbit to some degenerate equilibrium of (2), which itself is assumed to bifurcate in a reversible pitchfork bifurcation. With no loss of generality moving this equilibrium to the origin we assume

Assumption 2.3. $f(0, 0) = 0$, and $\sigma\,(D_1 f(0, 0)) = \{0\} \cup \{\pm\mu\}$ where 0 is a double non-semisimple eigenvalue and $\mu \in \mathbb{R}^+$.

It is straightforward to describe the local bifurcation of 0 using centre manifold reduction. The Centre Manifold Theorem [6] allows us to study the local bifurcation in a family of reversible and $\mathbb{Z}_2$-symmetric vector fields on centre manifolds W^c_λ. To be more precise, let us consider the extended system

$$\begin{aligned} \dot{x} &= f(x, \lambda) \\ \dot{\lambda} &= 0 \end{aligned}$$

with an equilibrium $(x, \lambda) = (0, 0)$, possessing a three-dimensional centre manifold. This manifold is foliated into $\{\lambda = \text{const.}\}$-slices which can be chosen such that the symmetries of (2) are preserved. The local bifurcation of 0 can be studied on these

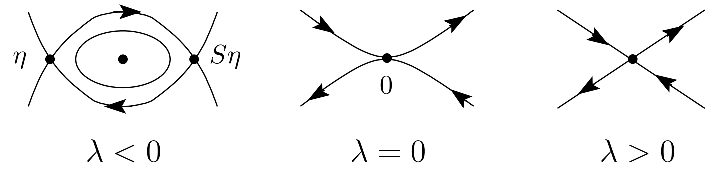

Figure 3. Phase portrait of the local bifurcation of 0 under assumption 2.4.

slices, and we denote them by W^c_λ. Note that this approach also introduces centre (un)stable manifolds $W^{cs(cu)}_\lambda$, which will be of interest below.

Assumption 2.3 generically leads to a local pitchfork bifurcation. This bifurcation can completely be studied by considering a normal form for the equilibrium, see [12]. We assume

Assumption 2.4. The local pitchfork bifurcation is of *eye type*. This means, that the normal form for the local bifurcation (after a centre manifold reduction) is given by

$$\dot{z}_1 = z_2, \quad \dot{z}_2 = \lambda z_1 + z_1^3. \tag{3}$$

where $z = (z_1, z_2)$ denote suitable coordinates in W^c_λ.

Remark. Essentially, we require the third order term in (3) to have positive sign. The case of negative sign describes the so-called *figure-eight* scenario in which two homoclinic orbits to 0 emerge in the local bifurcation. Reference [19] contains a study of the global bifurcation in this scenario. Here, however, we restrict to an analysis of the eye case. □

The action of the involutions R_i in W^c_λ (using (z_1, z_2)-coordinates) is given by $R_1 : (z_1, z_2) \to (z_1, -z_2)$ and $R_2 : (z_1, z_2) \to (-z_1, z_2)$. The phase portrait for the local bifurcation under assumption 2.4 can be easily derived and is given in figure 3. For $\lambda < 0$ two additional equilibria $\eta, S\eta \in \mathrm{Fix}\,(R_1)$ exist, which are connected by a symmetric heteroclinic cycle.

Our final assumption concerns the existence of a homoclinic orbit to 0.

Assumption 2.5. For $\lambda = 0$ there exists a homoclinic orbit $\Gamma = \{\gamma(t) : t \in \mathbb{R}\}$ to 0, i.e. $\gamma(t) \to 0$ as $t \to \pm\infty$. Moreover, $R_i\Gamma = \Gamma$ for $i = 1, 2$.

Recall from [17] that each symmetric orbit of an R-reversible system intersects the fixed space of R. Furthermore, there exists exactly one point of intersection when the orbit is not periodic. Therefore, the homoclinic orbit Γ intersects $\mathrm{Fix}\,(R_1)$ at some point, say $\gamma(0)$. We claim that $\gamma(0) \in \mathrm{Fix}\,(R_2)$. Indeed, it is straightforward to check that $R_2\gamma(0) \in \mathrm{Fix}\,(R_1)$ too. Since $\Gamma \cap \mathrm{Fix}\,(R_1)$ consists of a single point we conclude $R_2\gamma(0) = \gamma(0)$. Hence, $\gamma(0) \in \mathrm{Fix}\,(S)$ and the invariance of $\mathrm{Fix}\,(S)$ yields $\Gamma \subset \mathrm{Fix}\,(S)$. Moreover, since $W^c_\lambda \cap \mathrm{Fix}\,(S) = \{0\}$ the symmetries of Γ imply that the orbit is contained in the stable and unstable manifold of the 0 equilibrium.

We are interested in bifurcations from Γ as the parameter λ is varied. Observe first that the system (2), reduced to the invariant space $\mathrm{Fix}\,(S)$, is still reversible. We can therefore view Γ as a symmetric homoclinic orbit in a planar reversible system. Hence, Γ exists robustly for $\lambda \neq 0$. Nevertheless, because of the non-hyperbolicity of 0 at $\lambda = 0$ we expect to find homoclinic orbits bifurcating from Γ. In the next section we describe the approach to detect bifurcating one-homoclinic orbits to the centre manifolds W^c_λ, taken in [19].

3. Bifurcation of One-Homoclinic Orbits

In this section we review the results about the set of one-homoclinic orbits to the centre manifolds W^c_λ obtained in [19]. For this we consider the centre stable and centre unstable manifolds $W^{cs(cu)}_\lambda$ that have been obtained by the centre manifold reduction and globalise them along Γ. Homoclinic orbits to W^c_λ are then contained in the intersection $W^{cs}_\lambda \cap W^{cu}_\lambda$.

Let us introduce a cross section $\Sigma = \gamma(0) + Z$ to Γ at the point $\gamma(0)$. Note that Σ is three-dimensional and that it can be chosen such that it contains both $\mathrm{Fix}\,(R_1)$ and $\mathrm{Fix}\,(R_2)$, i.e. for the subspace Z we have $Z = \mathrm{Fix}\,(R_1) + \mathrm{Fix}\,(R_2)$. Parts of the manifolds $W^{cs(cu)}_\lambda$ will visit Σ many times. In a first step we consider the traces of the 'first' intersections of $W^{cs(cu)}_\lambda$ with Σ and investigate the existence of one-homoclinic orbits to W^c_λ. Exploiting the symmetries of (2) the following result has been proved in Lemmas 2.2 and 3.7 in [19].

Lemma 3.1. *For λ sufficiently close to* 0

- *the intersection of W^{cs}_λ and W^{cu}_λ at $\gamma(0)$ is non-transverse,*
- $\left(W^{cs(cu)}_\lambda \cap \Sigma\right) \pitchfork \mathit{Fix}\,(R_i)$ *in Σ for $i = 1, 2$.*

It is straightforward to interpret this lemma in terms of homoclinic orbits to W^c_λ. The important result is formulated as a theorem.

Theorem 3.2. *For each λ sufficiently close to 0 and for $i = 1, 2$ there exists a one-parameter family of R_i-symmetric homoclinic orbits to W^c_λ.*

The geometric approach has been made rigorous by a generalised version of Lin's method in [19]. Let us for later purposes present the analytical version of the above result. By lemma 3.1 we can represent the traces $W^{cs(cu)}_\lambda \cap \Sigma$ as graphs of functions $h^{cs(cu)}_\lambda$ over their common tangent space, say Y^c. Moreover, we can introduce coordinates $y_c = (y_1, y_2)$ in Y^c such that y_i represents the $\mathrm{Fix}\,(R_i)$ component in Y^c. Computations of Melnikov type then show that the difference $\xi_\lambda(y_c) := h^{cu}_\lambda(y_c) - h^{cs}_\lambda(y_c)$ can generically be expressed as

$$\xi_\lambda(y_c) = y_1 \cdot y_2, \tag{4}$$

independent of λ. In this setting the line $\{y_i = 0\}$ precisely corresponds to the family of R_i-symmetric homoclinic orbits to W^c_λ.

The asymptotic behaviour of the homoclinic orbits to W^c_λ can be studied in detail using the invariant foliation of the centre unstable manifolds W^{cu}_λ. Recall that for each

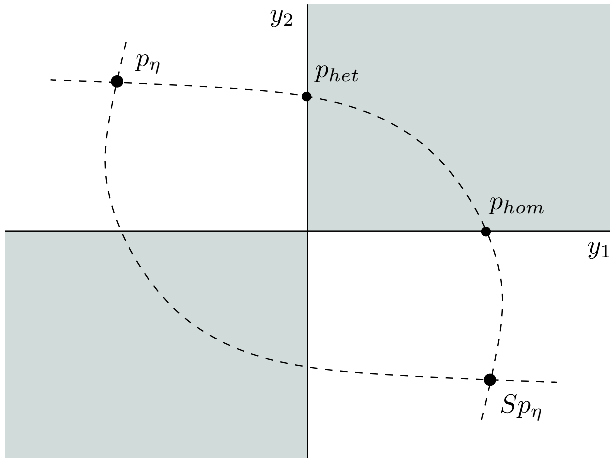

Figure 4. Generic position of the projection of the heteroclinic cycle between η, $S\eta$ along stable fibres in $W^{cs}_\lambda \cap \Sigma$ for $\lambda < 0$. The domain of the Poincaré map $\mathcal{P}$ is shown in grey. The y_i coordinates denote the $\mathrm{Fix}\,(R_i)$ component in Y^c.

λ the manifold W^{cu}_λ is foliated into unstable fibres, that is, from each point $z \in W^c_\lambda$ there originates a one-dimensional fibre $M_{z,\lambda}$, such that

$$W^{cu}_\lambda = \bigcup_{z \in W^c_\lambda} M_{z,\lambda},$$

see for instance [16]. The fibres depend smoothly on z and λ, and since the primary homoclinic orbit $\Gamma = M_{0,0}$ intersects Σ transversally we conclude that the *projection along fibres* is a smooth and injective map from W^c_λ to $W^{cu}_\lambda \cap \Sigma$. Moreover, the fibres enjoy an important invariance relation: Denoting the flow of (2) by $\phi_t(\cdot)$ we find that $\phi_t(M_{z,\lambda}) \subset M_{\phi_t(z),\lambda}$ for $t < 0$.

The projection along unstable fibres can be used relate the dynamics in W^c_λ to the situation in Σ and to obtain 'pictures' in $W^{cu}_\lambda \cap \Sigma$ of orbits in W^c_λ. For $\lambda < 0$ (which is the parameter range of interest) such a picture is shown in figure 4. For simplicity W^{cu}_λ is flattened out in this figure. The points p_η and Sp_η denote the points of intersection of the *strong unstable* manifold of η, $S\eta$ with $W^{cu}_\lambda \cap \Sigma$. It is important to note that generically these manifolds do not intersect $\mathrm{Fix}\,(R_i)$ since this would correspond to orbit-flip homoclinic (or heteroclinic) orbits, meaning orbits that approach the equilibrium along the *strong (un)stable* direction. Thus, figure 4 shows a generic picture.

Besides the points p_η and Sp_η the figure also contains an illustration of the projection of the (small) heteroclinic cycle between η, $S\eta$ in W^c_λ. A straightforward application of the invariance property of the fibres shows that the projected cycle is nothing but part of the traces of the unstable manifolds of η, $S\eta$ in Σ. Thus, we find that for $\lambda < 0$ these unstable manifolds intersect both $\mathrm{Fix}\,(R_1)$ and $\mathrm{Fix}\,(R_2)$ in Σ. Consequently, we obtain

Theorem 3.3. *For $\lambda < 0$ the families of homoclinic orbits to W^c_λ contain R_1-symmetric* *homoclinic orbits to η and $S\eta$ and an R_2-symmetric heteroclinic cycle between these equilibria.*

In the same way figure 4 reveals the existence of families of R_i-symmetric homoclinic orbits to periodic orbits in W^c_λ.

4. Existence of Two-Homoclinic Orbits

The existence of symmetric two-homoclinic orbits to W^c_λ, i.e. homoclinic orbits to W^c_λ intersecting Σ twice, is investigated by studying intersections of W^{cu}_λ with $\mathrm{Fix}\,(R_i)$ near 0. For this we consider the time evolution of points in $W^{cu}_\lambda \cap \Sigma$ and investigate the intersection of orbits with the fixed spaces $\mathrm{Fix}\,(R_i)$ in a local three-dimensional section Σ_0 near 0. This is achieved by studying a Poincaré map $\mathcal{P} : \mathrm{dom}\,\mathcal{P} \subset \Sigma \to \Sigma_0$, where $\mathrm{dom}\,\mathcal{P}$ denotes the domain of $\mathcal{P}$. We concentrate on parameter values $\lambda < 0$ in the following.

4.1. Definition of $\mathcal{P}$

For the definition and analysis of $\mathcal{P}$ we use suitable coordinates near 0. We introduce local coordinates (x_s, x_u, z_1, z_2) in some neighbourhood $\widehat{U}$ of 0 such that

$$W^{cs}_\lambda = \{x_u = 0\}, \quad W^{cu}_\lambda = \{x_s = 0\}, \quad W^c_\lambda = \{x_s = x_u = 0\}.$$

In [3] Deng proves that it is always possible to choose *admissible variables* in which the local (un)stable fibres are flattened out as well. Hence, with no loss of generality we can assume that the local stable fibre with base point $\hat{z} = (\hat{z}_1, \hat{z}_2) \in W^c_\lambda$ is given by $M_{\hat{z},\lambda} = \{x_u = 0, z = \hat{z}\}$. We can choose local coordinates such that the reversibility of the system is preserved. System (2) then reads in $\widehat{U}$

$$\begin{aligned} \dot{x}_s &= -\mu x_s + f_s(x_s, x_u, z, \lambda), \quad \dot{x}_u = \mu x_u + f_u(x_s, x_u, z, \lambda), \\ \dot{z} &= g(z, \lambda) + f_c(x_s, x_u, z, \lambda), \end{aligned} \tag{5}$$

with nonlinear terms f_s, f_u, f_c satisfying

$$Df_s(0,0,0,0) = 0, \ Df_u(0,0,0,0) = 0, \ Df_c(0,0,0,0) = 0,$$

and

$$\begin{aligned} f_s(0, x_u, z, \lambda) &= 0, & f_u(x_s, 0, z, \lambda) &= 0, \\ f_c(0, x_u, z, \lambda) &= 0, & f_c(x_s, 0, z, \lambda) &= 0. \end{aligned}$$

The vector field g is given in (3). With $z = (z_1, z_2)$ as coordinates in W^c_λ the involutions R_i act as

$$\begin{aligned} &R_1 : (x_s, x_u, z_1, z_2) \to (x_u, x_s, z_1, -z_2), \\ &R_2 : (x_s, x_u, z_1, z_2) \to (x_u, x_s, -z_1, z_2). \end{aligned}$$

Set $\Sigma_0 := \{x = (x_s, x_u, z_1, z_2) : x_s = x_u\}$. Then Σ_0 contains both $\mathrm{Fix}\,(R_1)$ and $\mathrm{Fix}\,(R_2)$, i.e. we have $\Sigma_0 = Z$. Moreover, $W^c_\lambda \subset \Sigma_0$ and a straightforward computation using (5) shows that orbits that pass by W^c_λ intersect Σ_0 transversally.

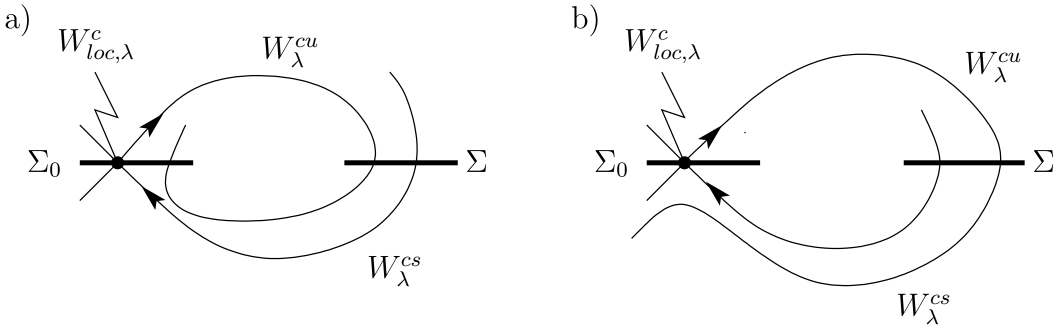

Figure 5. Schematic description of the domain of $\mathcal{P}$: If $\widetilde{W}^{cs}_\lambda$ is not twisted, then the part of W^{cu}_λ that starts inside W^{cs}_λ in Σ will intersect Σ_0 and eventually return to Σ (panel a)). Points outside W^{cs}_λ are not transported back to Σ (panel b)). Two dimensions are missing in this picture.

Let us now consider the solution $x_p(\cdot)$ through some point $p \in W^{cu}_\lambda \cap \Sigma$ such that $x_p(0) = p$, and assume that there exists a time $\tau \in \mathbb{R}^+$ such that $x(\tau) \in \Sigma_0$. If the orbit visits Σ_0 more than once then take τ as the smallest time. The assignment $p \mapsto x_p(\tau)$ defines a map

$$\mathcal{P} : \operatorname{dom} \mathcal{P} \to \Sigma_0,$$

where $\operatorname{dom} \mathcal{P}$ denotes the domain of $\mathcal{P}$.

We can characterise $\operatorname{dom} \mathcal{P}$ using formula (4). Recall that we are interested in orbits in W^{cu}_λ that start in Σ, intersect Σ_0, and return to Σ. Since $\dim W^{cs}_\lambda = 3$, this manifold divides the four-dimensional phase space. Therefore, as figure 5 illustrates, orbits that should return to Σ have to start on one distinguished side of W^{cs}_λ in Σ. More precisely, we can identify $W^{cs}_\lambda \cap \Sigma$ with W^c_λ by a projection along stable fibres, thereby obtaining a closed manifold $\widetilde{W}^{cs}_\lambda$. If this manifold is not twisted then the situation is as in figure 5: Exactly the points 'inside' $\widetilde{W}^{cs}_\lambda$ belong to $\operatorname{dom} \mathcal{P}$. On the other hand, if $\widetilde{W}^{cs}_\lambda$ is twisted $\operatorname{dom} \mathcal{P}$ is the set of points starting outside of this manifold in Σ.

We can distinguish which parts of W^{cu}_λ lie inside W^{cs}_λ in Σ using the graph representation of the traces of these manifolds introduced in the last section. Indeed, the geometric property can be expressed in terms of $h^{cs(cu)}_\lambda$-values of points in $W^{cs(cu)}_\lambda$ and points in $\operatorname{dom} \mathcal{P}$ are therefore characterised by the sign of ξ. Equation (4) thus implies that $\operatorname{dom} \mathcal{P} \cap W^{cu}_\lambda$ consists of two opposite quadrants in Y^c. We can distinguish two different cases, depending on whether the the points p_η, Sp_η, which are shown in figure 5, belong to $\operatorname{dom} \mathcal{P}$ or not. In this paper we deal with the latter case and assume

Assumption 4.1. Consider (2) with $\lambda < 0$ and let p_η, Sp_η denote the points in which the strong unstable manifolds of η, $S\eta$ intersect Σ. Then $p_\eta, Sp_\eta \notin \operatorname{dom} \mathcal{P}$.

In section 5 we will demonstrate numerically that assumption 4.1 is fulfilled for our introductory example. We also remark that in figure 4 the domain of $\mathcal{P}$ under assumption 4.1 is plotted in grey.

4.2. Analysis of $\mathcal{P}$

The existence of two-homoclinic orbits to W^c_λ is proved by considering the distinguished points p_{het}, p_{hom}, also shown in figure 4. Note that both points lie on the trace of the unstable manifold of η in Σ. Since $p_{het} \in \mathrm{Fix}\,(R_2)$ the orbit through this point will approach $S\eta$, whereas the orbit through $p_{hom} \in \mathrm{Fix}\,(R_1)$ approaches η as $t \to \infty$. Hence, the orbits through these points are homoclinic and heteroclinic orbits whose existence is asserted in theorem 3.3. In particular, this implies $p_{het}, p_{hom} \notin \mathrm{dom}\,\mathcal{P}$. But using estimates from [3] about the flow near W^c_λ we will show that there exist points in $\mathrm{dom}\,\mathcal{P}$ near p_{het} whose $\mathcal{P}$-image lies arbitrarily close to $S\eta$. Similarly, there exist points near p_{hom} whose $\mathcal{P}$-image lies arbitrarily close to η. Thus, the $\mathcal{P}$-images of curves in $\mathrm{dom}\,\mathcal{P}$ that connect such points near p_{het} with those near p_{hom} necessarily intersect $\mathrm{Fix}\,(R_2)$ in Σ_0, see figure 6 below. In this way we derive existence results for two-homoclinic orbits to W^c_λ.

Consider a point $p \in \mathrm{dom}\,\mathcal{P}$. We follow the solution $x_p(\cdot)$ of (2) with $x_p(0) = p$ until it intersects Σ_0 at some time τ_p. The corresponding trajectory is divided into two parts. The second part describes the behaviour of x_p in a neighbourhood of W^c_λ, the first one the behaviour outside this neighbourhood. For that let us introduce a box

$$B := \{(x_s, x_u, y) : |x_s| \leq \delta_1, |x_u| \leq \delta_1, ||z|| < \delta_2\}$$

where the δ_i are chosen such that $B \subset \widehat{U}$. The difficult task lies in describing the behaviour of solutions in B. Here it is of advantage that we are primarily interested in solutions that start close to W^{cs}_λ in Σ.

Consider the flight from Σ to B. For all $p \in \Sigma$ the orbit through p will enter B through the side $B_s := \{x_s = \delta_1\}$ of B. In particular, the primary homoclinic orbit Γ intersects B_s transversally. Thus, B_s is a cross section to the flow and therefore the corresponding map from Σ to B_s is a diffeomorphism. In particular, if $p \in W^{cs}_\lambda \cap \Sigma$, then there exists a time τ such that $x_p(\tau) = (\delta_1, 0, z_p)$. For orbits starting close to W^{cs}_λ we consequently obtain

Lemma 4.1. *If $p \in \Sigma$ is sufficiently close to W^{cs}_λ, then the orbit through p enters B in some point $(x_s, x_u, z) = (\delta_1, \varepsilon, z_p)$. Moreover, $\varepsilon \to 0$ as $d(p, W^{cs}_\lambda) \to 0$, where $d(\cdot,\cdot)$ denotes the Euclidean metric.*

The behaviour near 0 of solutions that enter B in points $(\delta_1, \epsilon, z_p)$ is essentially determined by the flow on the centre manifold W^c_λ. In fact, for solutions that start sufficiently close to W^{cs}_λ there is a time interval where both x_s and x_u are small. During this time interval the solution follows the flow in W^c_λ closely and hence the behaviour in W^c_λ determines where the solution intersects the cross section Σ_0.

This geometric consideration can be put on rigorous footing using general results by Deng [3] about the behaviour near nonhyperbolic equilibria. We can characterise any solution of interest to us by a *Shilnikov problem*, in that it fulfills

$$x_s(0) = \delta_1, \quad x_u(\tau) = \delta_1, \quad z(0) = \hat{z}. \tag{6}$$

In [3] Deng shows that given the *Shilnikov data* $(\tau, \delta_1, \delta_1, \hat{z})$ there exists a unique solution $(x_s, x_u, z)(t; \tau, \delta_1, \delta_1, \hat{z})$ of the Shilnikov problem (6) for equation (2). Moreover, he obtains *exponential expansions* for the solution. Let D^i denote the i-th derivative in all arguments of some function. We quote from Lemma 3.1 in [3]:

Lemma 4.2. *Let $(x_s, x_u, z)(\cdot)$ denote the (unique) solution of the above Shilnikov problem. Denote by z_c the solution in W^c_λ with $z_c(0) = \hat{z}$, and assume that this solution is bounded. Then there exists $\tilde{\mu} \in (0, \mu)$ and $K > 0$, such that for all $t \in [0, \tau]$ and $i = 0, 1, 2, \ldots$*

1) $|D^i x_s(t)| \leq K e^{-\tilde{\mu} t}$

2) $|D^i x_u(t)| \leq K e^{\tilde{\mu}(t-\tau)}$

3) $z(t) = z_c(t) + R(t)$, where $|D^i R(t)| \leq K e^{-\tilde{\mu}\tau}$.

This lemma can be used as follows. Let us once more consider a solution $(x_s, x_u, z)(\cdot)$ which enters B sufficiently close to W^{cs}_λ. The time τ this solution spends in B can be controlled by the distance to W^{cs}_λ. In particular, this distance determines at what time $\hat{\tau} \approx \tau/2$ the solution intersects Σ_0. During its passage through B there is a time interval where both x_s and x_u are exponentially small in τ, and z follows its reference solution z_c in W^c_λ exponentially closely according to points 1)-3) in lemma 4.2. With regard to our original problem concerning the Poincaré map we conclude that the solution intersects Σ_0 in an arbitrarily small neighbourhood of the position of the reference solution z_c, see estimate 3) in lemma 4.2.

We are now in position to prove the existence of points near p_{hom}, p_{het} whose $\mathcal{P}$-images lie in a neighbourhood of $R_2\eta$ and η, respectively.

Lemma 4.3. *For each $\varepsilon > 0$ there exist points p_1, p_2 (depending on ε) in the same quadrant of dom$\mathcal{P}$, such that $d(\mathcal{P}p_1, \eta) < \varepsilon$, $d(\mathcal{P}p_2, R_2\eta) < \varepsilon$ in Σ_0.*

Proof. We describe how to find the point p_1. For that we follow the solution through the distinguished point $p_{hom} \in W^{cs}_\lambda$ in Σ, see again figures 4 and 6. This point enters the box B at some point $(x_s, x_u, z) = (\delta_1, 0, z_r)$. Since the local stable fibres are flattened out in $\widehat{U} \supset B$, the solution z_c with $z_c(0) = z_r$ describes the small heteroclinic orbit, say Γ_h, from $R_2\eta$ to η that is contained in W^c_λ. We consider solutions through points $(x_s, x_u, z) = (\delta_1, \Delta, z_c(s))$, with $s \in (-1, 1)$. If $\Delta = 0$ all of these points lie on stable fibres of the orbit Γ_h. According to the above results we thus find that, given an ε-neighbourhood U of η, there exists a Δ such that every orbit through points $(\delta_1, \Delta, z_c(s))$ intersects Σ_0 in U.

It remains to show that there exists a point in dom$\,\mathcal{P}$ that enters B at a point of the form $(\delta_1, \Delta, z_c(s))$. This can be achieved by following solutions through these points backward to the cross section Σ. If $\Delta = 0$ the solutions intersect Σ in some curve which is contained in $W^{cs}_\lambda \cap \Sigma$ and transversally intersects $W^{cu}_\lambda \cap \Sigma$ in p_{hom}. Applying lemma 4.1 we conclude that for $\Delta \neq 0$ small the 'backward image' of $\{(\delta_1, \Delta, y_c(s)), s \in (-1, 1)\}$ also intersects W^{cu}_λ at some point p_1. Furthermore, for $\Delta > 0$ this point belongs to dom$\,\mathcal{P}$ and his $\mathcal{P}$-image is ε-close to η, by construction.

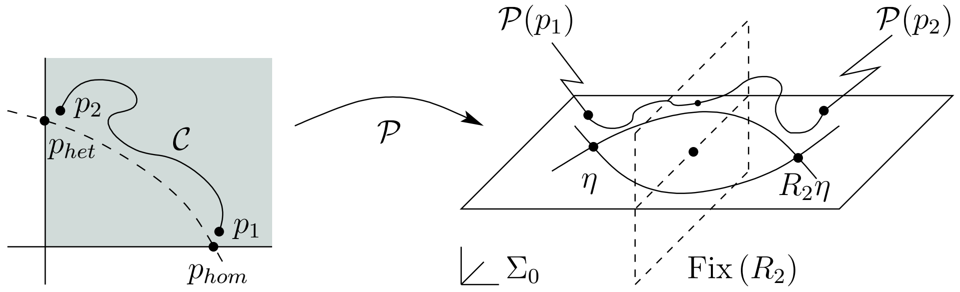

Figure 6. Existence of two-homoclinic orbits to W^c_λ. The left part shows a quadrant of dom $\mathcal{P}$ in Σ. The $\mathcal{P}$-image of curves through p_1 and p_2 must intersect Fix (R_2) in Σ_0, as shown in the right part. The intersection point represents a two-homoclinic orbit to W^c_λ.

The existence of p_2 is proved similarly using the distinguished point p_{het}. □

Let us now choose $\varepsilon > 0$ sufficiently small and take points p_1, p_2 according to the above lemma. We can connect these points by some curve $\mathcal{C}$ in dom $\mathcal{P}$. By continuity, $\mathcal{P}(\mathcal{C})$ is a curve in Σ_0 with end points $\mathcal{P}(p_i)$ on different sides of Fix (R_2). Therefore $\mathcal{P}(\mathcal{C})$ has to intersect Fix (R_2) in Σ_0, giving rise to an R_2-symmetric homoclinic orbit to W^c_λ, see figure 6. Moreover, we can choose an arbitrary curve $\mathcal{C}$ in $W^{cu}_\lambda \cap \text{dom}\,\mathcal{P}$ connecting p_1 and p_2 and consequently a one-parameter family of two-homoclinic orbits to W^c_λ exists.

Theorem 4.4. *Consider (2) with $\lambda < 0$, under the assumptions of section 2 and assumption 4.1. There exists a one-parameter family of R_2-symmetric two-homoclinic orbits to W^c_λ.*

Remark. Generically the intersection $W^{cu}_\lambda \cap \text{Fix}\,(R_2)$ is transverse and therefore one-dimensional. Consequently, a single one-parameter family of R_2-symmetric homoclinic orbits to W^c_λ exists generically. □

Just as in the case of one-homoclinic orbits in [19] we can refine this existence result. It is immediate that the family of two-homoclinic orbits contains two-homoclinic orbits to periodic solutions in W^c_λ. Moreover, by choosing a special curve $\mathcal{C}$ we can prove the existence of further connecting orbits between η, $R_2\eta$. Indeed, we find parts of the unstable manifold of η, $R_2\eta$ in dom $\mathcal{P}$. These parts stem from the projected heteroclinic cycle in W^{cu}_λ, see for instance figure 4 again. We can take $\mathcal{C}$ as the part between p_{het} and p_{hom} in figure 4 and conclude by the same argument as above that an orbit in the unstable manifold of η ($R_2\eta$) intersects Fix (R_2) near 0. Therefore a two-heteroclinic cycle between these equilibria exists.

Theorem 4.5. *In the setting of theorem 4.4 above there exists a two-heteroclinic cycle between the equilibria η, $R_2\eta$.*

In the next section we illustrate the last theorem by numerically computing two-heteroclinic solutions (and more) of the introductory example (1).

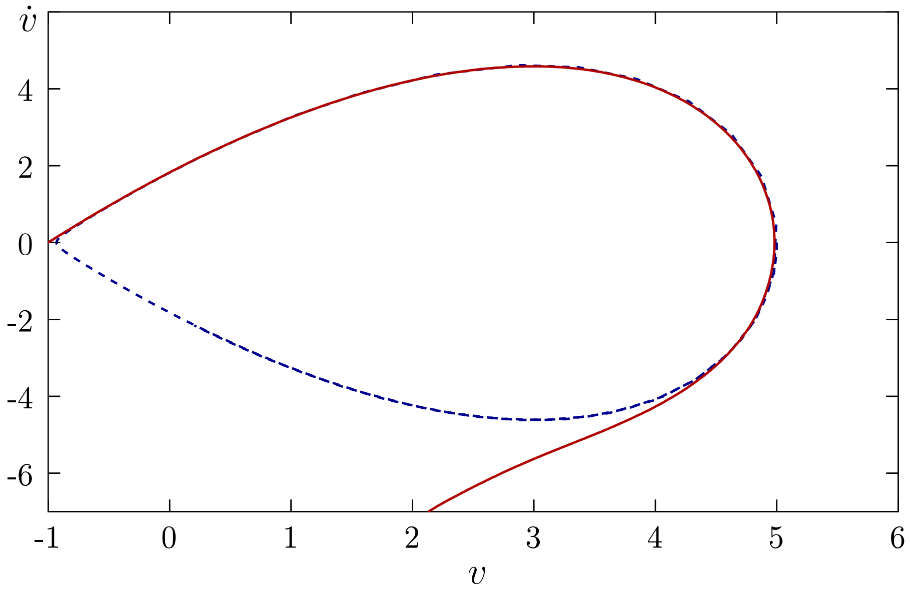

Figure 7. Behaviour of the strong stable manifold of ξ_3 at $\kappa = -3.001$. The plot shows the projection of a linear approximation to this manifold in $(v, \dot{v})$-space. The projection of the primary homoclinic orbit γ_{hom} is plotted dotted.

5. Further numerical studies

We return to the example (1) and illustrate the theory through numerical computations. As in the introductory part we use AUTO/HomCont and in particular a branch switching method for the detection of N-homoclinic orbits recently developed by Oldeman et.al. [14].

Before we present results about N-homoclinic and heteroclinic orbits for (1) we verify numerically that the theory so far applies to the system by showing that assumption 4.1 is fulfilled. For this we have to compute the strong unstable manifolds of the outer equilibria $\xi_{3,4} = (\pm\sqrt{-3-\kappa}, 0, -1, 0)$. (As in the introductory example above we consider the system (1) in $(v, \dot{v}, w, \dot{w})$-phase space with $\mu = 1$.) This can be accomplished by simple integrations of initial value problems with initial values obtained as linear approximations to the corresponding local strong unstable manifolds. It is obviously sufficient to restrict the computations to ξ_3.

We have solved the initial value problem using the Dormand-Prince method of order 5(4) as provided by MATLAB. The results show that the strong unstable manifold indeed satisfies assumption 4.1, in that there does not exist a cross section to the orbit γ_{hom} which is intersected by this manifold twice. In figure 7 we show the strong unstable manifold of ξ_3 at $\kappa = -3.001$. In accordance with figure 5 the solutions in figure 7 are projected onto $(v, \dot{v})$-space, which corresponds to the (x_s, x_u)-space in this example.

The preceding theory should therefore apply to system (1). As an illustration of the theory we compute N-heteroclinic and N-homoclinic orbits of the system that emerge in the reversible homoclinic pitchfork bifurcation at $\kappa = -3$. For this we have used a homoclinic branch-switching method recently developed by Oldeman et. al. in [14]. This method allows one very conveniently to compute N-homoclinic orbits in a neighbourhood of a given (numerically known) homoclinic solution.

The results suggest that a rich dynamics is created in the reversible homoclinic pitchfork bifurcation. Beside a 2-heteroclinic cycle between $\xi_{3,4}$ we could compute a variety of connecting solutions. Note that the branch-switching has only been coded for the detection of N-homoclinic solutions. We can, however, use again the reversing symmetry of (1) to compute also N-heteroclinic orbits.

In a first step we have computed N-homoclinic orbits to ξ_3 using the one-homoclinic orbit which emerges in the homoclinic pitchfork bifurcation as starting solution for the branch switching. The computations have been performed at $\kappa = -3.2$ for $N = 2, \ldots, 5$ and have shown that for these values a unique N-homoclinic orbit to ξ_3 exists. Continuation of these orbits in parameter space suggests that they are indeed created in the reversible homoclinic pitchfork bifurcation at $\kappa = -3$.

In the upper panel of figure 8 and figure 9 we give an impression of the computed two- and three-homoclinic solution at $\kappa = -3.5$. Projections of the orbits in phase space are not very enlightening this time; so we rather present the v- and w-component of the solutions.

It is interesting to consider the figures more closely. We see that the solutions first follow the one-homoclinic solution to ξ_3 until they approach $\mathrm{Fix}\,(S)$ $(v = 0)$. Then they follow γ_{hom} twice before they return to ξ_3. The solutions are therefore not N-homoclinic in the classic sense since they are composed of two homoclinic solutions to different equilibria. But along the lines of this paper it is perfectly justified to view them as N-homoclinic solutions to the centre manifold.

For the computation of N-heteroclinic cycles between ξ_3 and ξ_4 we have again exploited the reversing symmetry of (1). We have continued the N-homoclinic solutions very close to the critical parameter value $\kappa = -3$. Then we have only considered the first half of the solution running from the equilibrium to the fixed space $\mathrm{Fix}\,(R_1)$. (Note that the 'middle point' of each N-homoclinic orbit computed above lies close to either $\gamma_{hom}(0)$ or ξ_2, and therefore close to $\mathrm{Fix}\,(R_2)$.) For each $N = 2, \ldots, 5$ it has been possible to continue this part as an R_2-symmetric solution which shows the existence of such N-heteroclinic cycles between ξ_3 and ξ_4. The lower panels of figure 8 and figure 9 give an impression of the corresponding heteroclinic solutions. The similarity to the N-homoclinic orbits computed before is apparent, but also not surprising because of the way the orbits have been computed.

6. Conclusions

In this paper we have continued the study of the reversible homoclinic pitchfork bifurcation begun in [19] and have proved the existence of a family of two-homoclinic orbits to W^c_λ which in particular contains a two-heteroclinic cycle between equilibria.

The analytical studies have been illustrated by numerical investigations on a system

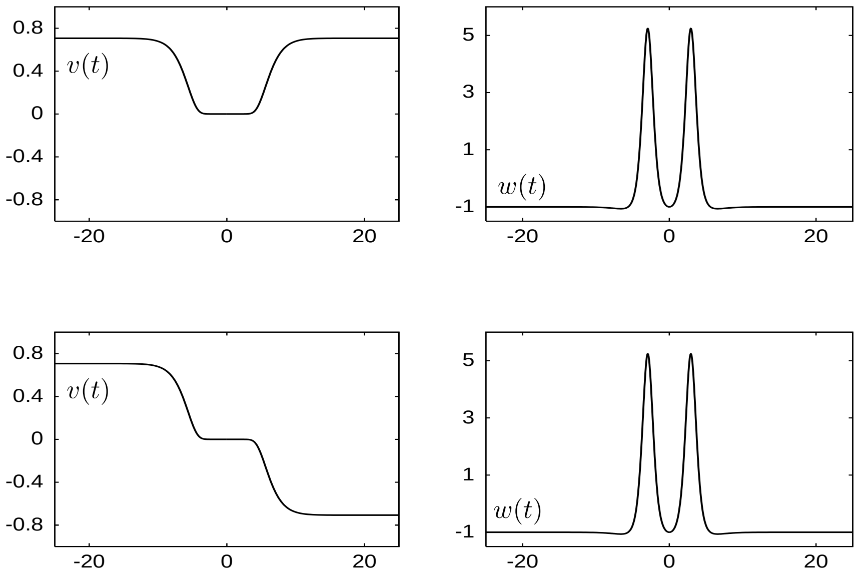

Figure 8. Two-homoclinic and two-heteroclinic solutions of (1). Figures show the v- and w-component of the solution computed by the procedure described in the text for $\kappa = -3.5$.

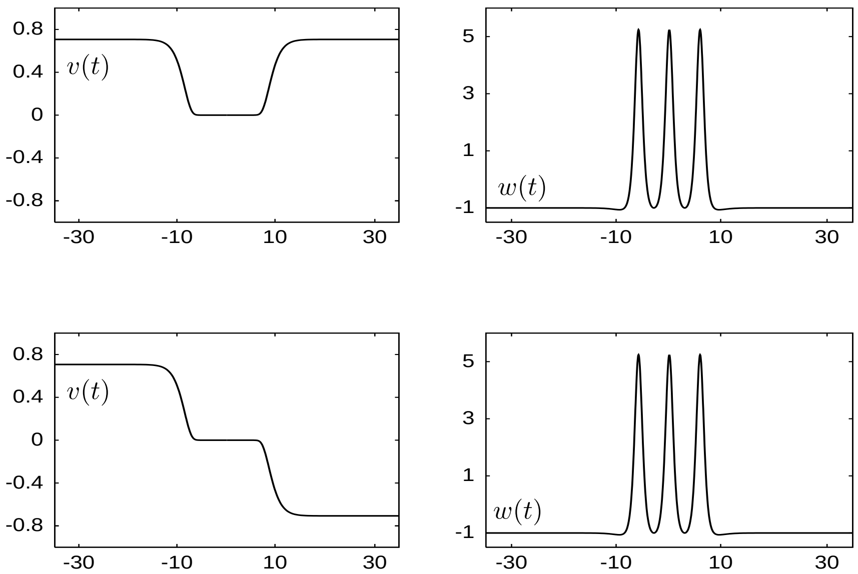

Figure 9. Three-homoclinic and three-heteroclinic solutions of (1). Figures show the v- and w-component of the solution computed by the procedure described in the text for $\kappa = -3.5$.

of second-order ODEs (1), where a variety of N-homoclinic and N-heteroclinic orbits has been found to bifurcate from the primary orbit. We note that the system (1) is also Hamiltonian. However, for the general analysis we considered the class of reversible and $\mathbb{Z}_2$-symmetric systems, because similar to the results in [19] we have found these symmetries to be the most important influence for the dynamics. Indeed, if one would consider the bifurcation in the class of reversible Hamiltonian systems instead, then the primary homoclinic connection can break under perturbations. Hence, a second parameter is needed for an unfolding of the situation such that we deal with a codimension-two bifurcation. Results about the bifurcation of one-homoclinic orbits in this case have been derived in [20].

Nevertheless, it would be interesting to analyse how the property of (1) being Hamiltonian can be incorporated in the present analysis. The existence of N-homoclinic orbits in Hamiltonian systems is well understood in a number of scenarios. Classic studies have concerned N-homoclinic orbits to hyperbolic equilibria in the neighbourhood of a given primary homoclinic orbit, [4, 22]. Note that most of the results are also valid (in an often slightly weaker version, however) for reversible systems, see [1] and references therein.

More recently research interests have shifted to N-homoclinic orbits emerging in the bifurcation of homoclinic orbits to nonhyperbolic equilibria. In particular, the case of homoclinic orbits to saddle-centres has been studied in [13], see also [2] for a collection of results about this bifurcation in reversible systems. Investigations in [11, 10] have dealt with the bifurcation of homoclinic orbits to the corresponding centre manifolds. In [19, 20] and in the present paper we have generalised this approach to the case of degenerate equilibria.

Related studies about homoclinic orbits to invariant manifolds have been undertaken for singularly perturbed equations and nearly-integrable Hamiltonian systems, see [8, 7] and references therein. The mainly geometrical analysis in those papers concerns homoclinic orbits to *slow manifolds*, which play the same role as the centre manifold in our analysis. We also note that variational methods have been successfully used to prove the existence of N-homoclinic orbits for several classes of (possibly time-dependent) Hamiltonian systems; for an overview see [15]. Note, however, that our main goal is to gain insight into the dynamics of the reversible homoclinic pitchfork bifurcation, rather than to derive mere existence results for N-homoclinic orbits.

Our analysis in this paper has revealed the difficulties of a geometric approach, which can quickly become involved and is only suitable for a limited range of problems. In fact, most of the analysis in section 4 is designed specifically for the bifurcation studied here and can hardly be generalised to other scenarios. The main reason for the difficulties lies in the still incomplete description of the dynamics near W^c_λ and the principal problem to track orbits geometrically because of the nontrivial dynamics in W^c_λ.

The main challenge therefore lies in turning the geometric ideas of section 4 into an analytical theory, which could be applied to other - probably more relevant - examples from nonlinear optics and water wave theory, where similar scenarios have been found in [20]. We finally note that another interesting aspect of the dynamics in the reversible homoclinic pitchfork bifurcation is the occurrence of so-called bellows structures, formed by homoclinic orbits and heteroclinic cycles. In [9] these bellows have been proved to be sources of a rich dynamical behaviour. Note that already our results about 2-homoclinic orbits in the reversible homoclinic pitchfork bifurcation show differences to the results in [9], since it has been proved there that homoclinic bellows are generically not accompanied by N-homoclinic orbits.

Acknowledgements

The main part of the paper has been originally contained in the author's PhD Thesis [21]. He greatly acknowledges many fruitful discussions with Jürgen Knobloch and thanks for a careful reading of the original manuscript.

References

[1] Champneys A R 1998 Homoclinic orbits in reversible systems and their applications in mechanics, fluids and optics *Physica D* **112** 158-186

[2] Champneys A R 1999 Homoclinic orbits in reversible systems II: Multi-bumps and saddle-centres *CWI Quarterly* **12** 185-212

[3] Deng B 1990 Homoclinic bifurcations with nonhyperbolic equilibria *SIAM J. Math. Anal.* **21** 693–720

[4] Devaney R L 1976 Homoclinic orbits in Hamiltonian systems *J. Diff. Eqns.* **21** 431-438

[5] Doedel E J, Champneys A R, Fairgrieve T R, Kuznetsov Yu A, Sandstede B and Wang X J 1997 AUTO97: Continuation and Bifurcation Software for Ordinary Differential Equations Available by anonymous ftp from FTP.CS.CONCORDIA.CA, directory PUB/DOEDEL/AUTO

[6] Guckenheimer J and Holmes P 1983 *Nonlinear Oscillations, Dynamical Systems and Bifurcations of Vector Fields* (New York: Springer)

[7] Haller G and Wiggins S 1995 N-pulse homoclinic orbits in perturbations of resonant Hamiltonian systems *Arch. Rational Mech. Anal.* **130** 25-101

[8] Holmes P, Doelman A, Hek G M and Domokos G 2001 Homoclinic orbits and chaos in three- and four-dimensional flows *Phil. Trans. Roy. Soc. Lond. A* **359** 1429-1438

[9] Homburg A J and Knobloch J 2004 Multiple homoclinic orbits in conservative and reversible systems *Transactions of the AMS*, to appear

[10] Klaus J and Knobloch J 2003 Bifurcation of homoclinic orbits to a saddle-center in reversible systems *Int. J. Bifurcation Chaos* **13** 2603-2622

[11] Koltsova O Yu and Lerman L M 1996 Families of transverse Poincaré homoclinic orbits in $2N$-dimensional Hamiltonian systems close to the system with a loop to a saddle-center *Int. J. Bifurcation Chaos* **6** 991-1006

[12] Lamb J S W and Capel H W 1995 Local bifurcations on the plane with reversing point group symmetry *Chaos, Solitons and Fractals* **5** 271–293

[13] Mielke A, Holmes P and O'Reilly O 1992 Cascades of homoclinic orbits to, and chaos near, a Hamiltonian saddle-center *J. Dynamics Diff. Eqns.* **4** 95-126

[14] Oldeman B E, Champneys A R and Krauskopf B 2003 Homoclinic branch switching: a numerical implementation of Lin's method *Int. Journal of Bifurcation and Chaos* **13** 2977-3000

[15] Rabinowitz P H 1996 Multibump solutions of differential equations: overview *Chinese Journal of Mathematics* **24** 1-36

[16] Shilnikov L P, Shilnikov A L, Turaev D V and Chua L O 1998 *Methods of Qualitative Theory in Nonlinear Dynamics. Part I* (Singapore: World Scientific)

[17] Vanderbauwhede A and Fiedler B 1992 Homoclinic period blow-up in reversible and conservative systems *Z. Angew. Math. Phys.* **43** 292–318
[18] Wagenknecht T 2002 Bifurcation of a reversible Hamiltonian system from a fixed point with fourfold eigenvalue zero *Dynamical Systems* **17** 29–45
[19] Wagenknecht T 2002 About a homoclinic pitchfork bifurcation in reversible systems with additional $\mathbb{Z}_2$-symmetry *Nonlinearity* **15** 2097–2119
[20] Wagenknecht T and Champneys A R 2003 When gap solitons become embedded solitons: a generic unfolding *Physica D* **177** 50–70
[21] Wagenknecht T 2004 Homoclinic Bifurcations in Reversible Systems *PhD Thesis* TU Ilmenau
[22] Wiggins S 1988 Global Bifurcations and Chaos : Analytical Methods (New York: Springer)